Fisetin ameliorates atherosclerosis by regulating PCSK9 and LOX-1 in apoE$^{-/-}$ mice

LI YAN*, QINGLING JIA*, HUI CAO, CHUAN CHEN, SANLI XING, YAN HUANG and DINGZHU SHEN

Shanghai Geriatric Institute of Chinese Medicine, Shanghai University of Traditional Chinese Medicine, Shanghai 200031, P.R. China

Received March 31, 2020; Accepted September 22, 2020

DOI: 10.3892/etm.2020.9457

Abstract. The purpose of the current study was to investigate the mechanism by which fisetin improves atherosclerosis (AS) by regulating lipid metabolism and senescence in apolipoprotein E-deficient (apoE$^{-/-}$) mice. An AS model was established by feeding apoE$^{-/-}$ mice a high-fat diet. Mice were randomly divided into the model group (n=18), the fisetin group (n=18) and the atorvastatin group (n=18). The control group (n=18) was composed of wild-type C57BL/6 mice of the same age and genetic background. The fisetin and atorvastatin groups were respectively treated with aqueous solutions of fisetin (12.5 mg/kg) and atorvastatin (2 mg/kg) via oral gavage daily for 12 weeks. The pathological morphology, lipid accumulation, collagen deposition of the aortic sinus were observed, serum lipids, superoxide dismutase (SOD) and malondialdehyde (MDA) levels and alanine aminotransferase (ALT) and aspartate aminotransferase (AST) activities were measured in the peripheral blood serum. Additionally, the expressions of proprotein convertase subtilisin/kexin type 9 (PCSK9), lectin-like oxidized low-density lipoprotein receptor-1 (LOX-1), tumor suppressor protein p53 (p53), cyclin-dependent kinase inhibitor 1A (p21) and multiple tumor suppressor-1 (p16) were analyzed in the aorta. The results of the current study indicated that compared with the control group, a large area of AS plaque in the aortic sinus that contained a large amount of red-stained lipids and decreased collagen fiber content were found in the model group, which exhibited higher total cholesterol (TC), low-density lipoprotein cholesterol (LDL-C), very low-density lipoprotein cholesterol (VLDL-C), oxidized low-density lipoprotein (ox-LDL) and MDA levels; higher ALT and AST activities, lower high-density lipoprotein cholesterol (HDL-C) and SOD levels and increased expression levels of PCSK9, LOX-1, p53, p21 and p16. Fisetin is a phytochemical and bioflavonoid that serves a potential role in chronic diseases including AS, obesity, diabetes and cancer due to its wide biological activities, such as regulating lipid metabolism and anti-aging, anti-oxidation and anti-inflammatory. Atorvastatin is recognized as a first-line treatment drug for AS; therefore it was used as a positive control in the current study. Following fisetin and atorvastatin treatment, both the AS plaque and the lipid accumulation in the aortic sinus were significantly reduced, and the expressions of PCSK9, LOX-1 and aging markers, including p53, p21 and p16 were downregulated.

Correspondence to: Dr Dingzhu Shen, Shanghai Geriatric Institute of Chinese Medicine, Shanghai University of Traditional Chinese Medicine, 365C Xiangyang South Road, Shanghai 200031, P.R. China
E-mail: 13818279131@163.com

*Contributed equally

Key words: fisetin, atherosclerosis, lipid metabolism, proprotein convertase subtilisin/kexin type 9, lectin-like oxidized low-density lipoprotein receptor-1

Introduction

Atherosclerosis (AS) is a multifactorial disease that is closely associated with aging and involves a number of lipid metabolism disorders (1). Proprotein convertase subtilisin/kexin type 9 (PCSK9) is a key regulator of cholesterol metabolism, can promote the degradation of plasma low-density lipoprotein receptor (LDLR) and increase the level of low-density lipoprotein cholesterol (LDL-C), leading to an increased risk of AS (2). Lectin-like oxidized low-density lipoprotein receptor-1 (LOX-1) is the main receptor of oxidized low-density lipoprotein (ox-LDL), which interacts with ox-LDL induced endothelial dysfunction, macrophage-derived foam cell formation and LOX-1 activation to promote the formation of atherosclerotic plaques and acute cardiovascular events (3). It has been previously reported that LOX-1 expression is enhanced by the overexpression of PCSK9 in human aortic endothelial cells (ECs), smooth muscle cells (SMCs) and mouse aorta, whereas the LOX-1 expression is reduced by silencing PCSK9 (4). Within patients with AS, free radicals and lipid peroxidation that is produced by lipid oxidation can cause cell necrosis and apoptosis (5). Tumor suppressor protein p53 (p53), cyclin-dependent kinase inhibitor 1A (p21), and multiple tumor suppressor-1 (p16) are associated with the cell cycle regulation, apoptosis and senescence, which are also associated with AS (6). A previous study demonstrated that low shear stress that is mediated by reactive oxygen species (ROS) can enhance the expression of PCSK9 in human ECs and SMCs, whereas silencing ROS can inhibit PCSK9 expression

and reduce the effect of LOX-1 (7). In addition, PCSK9 serves an important role in the process of vascular aging, which can aggravate endothelial dysfunction caused by oxidative stress and inflammation by stimulating LOX-1 in order to further accelerate the pathological changes of AS (8).

Fisetin (3,3',4',4,7-tetrahydroxyflavone) is a natural flavonoid molecule that can regulate abnormal lipid metabolism, anti-oxidation and anti-aging activities (9). Fisetin has been revealed to regulate obesity and cardiovascular disease by promoting the expression of adiponectin in 3T3-L1 preadipocytes (10). Fisetin can also effectively improve lipid metabolism, oxidative stress and liver injury in mice with metabolic syndrome that is induced by a high-fructose diet (11). In a previous study, fisetin was revealed to reduce the expression of p16 and p21 in progeroid *Ercc1*$^{-/\Delta}$ mice and aged wild-type mice, as well as in human adipose tissue senescent cells (12). Our previous study demonstrated that fisetin can limit ox-LDL-induced lipid accumulation and senescence in RAW264.7 macrophage-derived foam cells (13). Based on the previous study, the current study explored how fisetin may regulate lipid metabolism via PCSK9 and LOX-1 as well as improve the aging status of AS in apoE$^{-/-}$ mice. An AS model was established in apoE$^{-/-}$ mice, which was induced by a high-fat diet. The pathological morphology, lipid accumulation and collagen deposition of the aortic sinus was subsequently detected in mice. Additionally, serum levels of total cholesterol (TC), triglyceride (TG), high-density lipoprotein cholesterol (HDL-C), LDL-C, very low-density lipoprotein cholesterol (VLDL-C), ox-LDL, superoxide dismutase (SOD) and malondialdehyde (MDA), alanine aminotransferase (ALT) and aspartate aminotransferase (AST) activities were determined and PCSK9, LOX-1, p53, p21 and p16 expressions in the aorta were assessed.

Materials and methods

Experimental animals. In the current study, a total of 54 12-week-old specific pathogen-free (SPF) male apoE$^{-/-}$ mice [weight, 20±5 g; animal license no. SCXK (Jing) 2016-0010] and 18 wild-type male C57BL/6 mice of the same age and genetic background [animal license no. SCXK (Zhe) 2019-0001] were purchased from Beijing Vital River Lab Animal Technology Co., Ltd. The mice were kept in an SPF grade animal facility at the Shanghai Model Organisms Center, Inc. (Shanghai, China) at a room temperature of 19-22˚C, relative humidity of 50-70% and a 12 h light/dark cycle. All animals had free access to food and water, and experimental operations strictly followed the rules and regulations of the Shanghai Model Organisms Center, Inc. The protocol of the present study was approved by the Animal Care and Use Committee of the Shanghai Model Organisms Center, Inc. (IACUC no. 2019-0008).

Modeling and grouping. 54 apoE$^{-/-}$ 12-week-old mice were fed a normal diet for 1 week before being randomly divided into three groups: apoE$^{-/-}$ mice + high-fat diet (model group; n=18), apoE$^{-/-}$ mice + high-fat diet + fisetin (fisetin group; n=18) and the apoE$^{-/-}$ mice + high-fat diet + atorvastatin (atorvastatin group; n=18). The high-fat diet formula was a normal mouse diet (0.03% corn, 0.15% secondary meal, 0.03% alfalfa, 0.08% soybean meal, 0.07% Peru fish meal, 0.05% American chicken meal, 0.04% animal premix 1, 0.02% gluten, 0.005% calcium dihydrogen phosphate, 0.5% rice, 0.005% stone powder, 0.02% salad oil, 0.0045% feed grade sodium chloride and 0.0015% feed grade magnesium chloride) with the addition of 21% fat and 0.5% cholesterol. Wild-type C57BL/6 mice of the same genetic background and age were used as the controls (control group, n=18) and were fed a normal mouse diet. Mice in the fisetin and atorvastatin groups were gavaged with aqueous solutions of fisetin and atorvastatin, respectively. Via conversion with reference to an adult body weight of 60 kg and the equivalent dose of mice, the final doses of fisetin and atorvastatin aqueous solutions provided to mice were 12.5 and 2 mg/kg, respectively. The fisetin was dissolved in 0.1% DMSO aqueous solution, and the atorvastatin tablets as a positive control drug were directly dissolved in distilled water. The control and model groups were treated with the same volume (0.2 ml/mouse/day) of distilled water via daily oral gavage, and the intervention period of each group was 12 weeks.

Drugs and reagents. Fisetin (20 mg; cat. no. B20953) was purchased from Shanghai Yuanye Biotechnology Co., Ltd. Atorvastatin tablets (20 mg; cat. no. H20051408) were purchased from Pfizer, Inc. DMSO (cat. no. 472301) was obtained from Sigma Aldrich; Merck KGaA. The protein ladder (cat. no. 26616) was obtained from Thermo Fisher Scientific, Inc. The BCA Protein Assay kit (cat. no. P0010) and SDS-PAGE Gel Preparation kit (cat. no. P0012A) were purchased from Beyotime Institute of Biotechnology. Rabbit anti-PCSK9 (cat. no. ab95478), mouse anti-p53 (cat. no. ab26), rabbit anti-p21 (cat. no. ab188224) and rabbit anti-p16 (cat. no. ab51243) were purchased from Abcam. Mouse anti-LOX-1 (cat. no. AF1564) was supplied by R&D Systems, Inc. Rabbit anti-GAPDH (cat. no. 5174S), goat anti-rabbit IgG horseradish peroxidase (HRP)-conjugated secondary antibody (cat. no. 7074P2) and horse anti-mouse IgG HRP-linked secondary antibody (cat. no. 7076P2) were purchased from Cell Signaling Technology, Inc. Mouse TC (cat. no. Ek-M20591), mouse TG (cat. no. Ek-M20590), mouse HDL-C (cat. no. Ek-M20589), mouse LDL-C (cat. no. Ek-M20588), mouse VLDL-C (cat. no. Ek-M21066), mouse ox-LDL (cat. no. Ek-M21214), SOD (cat. no. Ek-M21269) and MDA (cat. no. Ek-M21268) ELISA kits were purchased from Ek-Bioscience Biotechnology Co., Ltd. An ALT Assay kit (cat. no. C009-2-1) and an AST Assay kit (cat. no. C010-2-1) were purchased from Nanjing Jiancheng Bioengineering Institute.

Hematoxylin and eosin (H&E), Oil Red O and Masson staining of the aortic sinus. Mice (36 apoE$^{-/-}$ mice and 12 C57BL/6 mice) were anesthetized by intraperitoneal injection of 2% pentobarbital sodium (50 mg/kg) and euthanized by infusion with 10% formalin. The heart and blood vessels between the thoracic aorta and abdominal aorta were removed and preserved in 10% formalin (fixed in 10% formalin at 4˚C for one day) for paraffinization or frozen sectioning, in which paraffin sections (thickness of sections: 5 μm) were used for H&E staining (hematoxylin staining solution, 5 min; eosin staining solution, 5 min; both room temperature) and Masson staining (Masson Stain kit, cat. no. D026-1-3; Nanjing Jiancheng Bioengineering Institute; nuclear staining solution

60 sec, slurry staining solution 60 sec, color separation solution 8 min, counterstain solution 5 min; all room temperature). Frozen sections (thickness of sections: 10-15 μm) were used for Oil Red O staining (Oil Red O solution; 10 min; room temperature), and the pathological morphology, lipid accumulation and collagen deposition of mice aorta were observed. The H&E and Masson staining images were observed using an optical microscope (BX51; Olympus Corporation; magnification, x40, x100, x200), and the Oil Red O staining images were acquired using a scanner (Panoramic MIDI; 3DHISTECH). The images were semi-quantitatively analyzed using Image-Pro Plus Version 6.0 (Media Cybernetics, Inc.) as follows: Plaque area ratio = plaque area/total aortic sinus lumen area; red-stained lipid area ratio=red-stained area/total aortic sinus lumen area; and collagen fiber content ratio = blue-stained area/total aortic sinus lumen area.

Detection of lipids, SOD, MDA levels and ALT and AST activities in the peripheral blood serum of mice. Mice (18 apoE$^{-/-}$ mice and 6 C57BL/6 mice) were anesthetized by intraperitoneal injection of 2% pentobarbital sodium (50 mg/kg) after being fasted for 12 h. Blood was collected from the retro-orbital plexus and mice were euthanized via cervical dislocation. Blood was then incubated at 4˚C for 12 h, and centrifuged at 13,523 x g at 4˚C for 30 min to absorb the serum. The serum levels of TC, TG, HDL-C, LDL-C, VLDL-C, ox-LDL, SOD and MDA were detected according to the instructions of the mouse TC, TG, HDL-C, LDL-C, VLDL-C, ox-LDL, SOD and MDA ELISA kits. The optical density (OD) value of each sample was measured at a wavelength of 450 nm. The activities of ALT and AST in the serum were detected according to the instructions of the ALT and AST Assay kits. The OD value of the sample was measured at a wavelength of 510 nm. The standard curve was drawn according to the manufacturer's instructions of mouse TC, TG, HDL-C, LDL-C, VLDL-C, ox-LDL, SOD, MDA ELISA kits and ALT, AST Assay kits, with the corresponding concentration range or activity obtained based on the standard curve.

Detection of PCSK9, LOX-1, p53, p21 and p16 protein expression in the aorta. After sampling blood from the retro-orbital plexus of mice, the blood vessels between the thoracic and abdominal aorta were immediately collected. The total protein of mouse aorta was extracted from aortic tissues with RIPA lysis buffer (cat. no. P0013B; Beyotime Institute of Biotechnology) containing PMSF (cat. no. ST506; Beyotime Institute of Biotechnology), samples were mixed with 5X loading buffer (cat. no. P0015; Beyotime Institute of Biotechnology) and quantified using the BCA Protein Assay kit. The proteins were separated by SDS-PAGE Gel Preparation kit (percentage of the gel, 12%; 80 V for 30 min followed by 120 V for 90 min), transferred to a PVDF membrane using the wet transfer method (270 mA for 90 min), and blocked with 5% skim milk at room temperature for 2 h. Membranes were then incubated overnight at 4˚C with rabbit anti-PCSK9 (74 kDa; 1:1,000), mouse anti-LOX-1 (52 kDa; 1:1,000), mouse anti-p53 (53 kDa; 1:1,000), rabbit anti-p21 (21 kDa; 1:1,000), rabbit anti-p16 (16 kDa; 1:1,000) and rabbit anti-GAPDH (37 kDa; 1:3,000). The membrane was washed three times (10 min each), incubated with the corresponding HRP-conjugated secondary antibody (1:3,000) for 1 h at room temperature and then washed three times additionally (10 min each). Luminescent solution A and liquid B were mixed 1:1 according to the instructions of the Tanon™ High-sig ECL Western Blotting Substrate kit (Tanon Science & Technology Co., Ltd.). The membrane was scanned using the iBright FL1000 Imaging System (Thermo Fisher Scientific, Inc). ImageJ 1.48v (National Institutes of Health) was used to analyze the integrated absorbance (IA) of the protein band (IA = average light density value*area). The relative expression level of the target protein was measured by dividing the IA of the target protein by the IA of GAPDH.

Statistical analysis. Statistical analysis was performed using SPSS 24.0 (IBM Corp.), and figures were created using GraphPad Prism 8.0.2 (GraphPad Software, Inc.), Adobe Illustrator CC 23.0.2 (Adobe Systems Inc.) and Adobe Photoshop CC 20.0.6 (Adobe Systems Inc.). Results are presented as the means ± standard deviation (mean ± SD). The differences among groups were analyzed using one-way ANOVA, followed by least-significant difference (LSD) test. Statistical analyses were two-tailed tests with α=0.05. $P<0.05$ was considered to indicate a statistically significant difference.

Results

Lipid levels. Compared with the control group, the levels of TC, LDL-C, VLDL-C, and ox-LDL increased in the model group, whereas the level of HDL-C decreased ($P<0.01$; Table I), and no statistically significant differences were observed in TG content. Compared with the model group, the mice in the fisetin and atorvastatin groups exhibited lower levels of TC, LDL-C, VLDL-C, and ox-LDL ($P<0.01$; Table I), but there were no significant differences in the levels of TG and HDL-C ($P>0.05$; Table I). Additionally, there were no significant differences between the fisetin and atorvastatin groups ($P>0.05$; Table I).

SOD and MDA levels. In the model group, SOD levels significantly decreased and MDA levels significantly increased compared with the control group ($P<0.001$; Table II). However, compared with the model group, SOD levels increased and MDA levels decreased in the fisetin and atorvastatin groups ($P<0.01$; Table II). There were no significant differences between the fisetin and atorvastatin groups ($P>0.05$; Table II).

ALT and AST activity. The activities of ALT and AST in the model group were significantly increased compared with the control group ($P<0.001$). However, in the fisetin and atorvastatin groups, the activities of ALT and AST were significantly lower compared to the model group ($P<0.001$; Table III). There were no significant differences between the fisetin and atorvastatin groups ($P>0.05$; Table III).

Detection of the aortic sinus plaque area. After the mice were fed with a high-fat diet for 12 weeks, a greater amount of atherosclerotic plaque formed in the aortic sinus compared with the control group ($P<0.001$; Fig. 1A and B). Compared with the model group, AS plaque significantly decreased in the fisetin and atorvastatin groups ($P<0.001$; Fig. 1A and B). There

Table I. Serum lipid levels in peripheral blood of mice in each group.

Group	n	TC (mmol/l)	TG (mmol/l)	LDL-C (mmol/l)	HDL-C (mmol/l)	VLDL-C (mmol/l)	ox-LDL (μg/ml)
Control	6	7.36±0.52	5.23±0.31	6.04±0.11	1.62±0.08	0.95±0.06	8.59±1.25
Model	6	8.24±0.33[a]	5.73±0.70	6.54±0.16[a]	1.51±0.04[a]	1.20±0.21[a]	10.16±0.29[a]
Fisetin	6	7.50±0.41[b]	5.36±0.21	6.19±0.35[b]	1.56±0.04	0.99±0.06[b]	8.95±0.50[b]
Atorvastatin	6	7.38±0.37[b]	5.31±0.22	6.14±0.11[b]	1.57±0.04	0.97±0.05[b]	8.88±0.33[b]

Data are presented as mean ± SD. [a]P<0.01 vs. control; [b]P<0.01 vs. model. TC, total cholesterol; TG, triglyceride; LDL-C, low-density lipoprotein cholesterol; HDL-C, high-density lipoprotein cholesterol; VLDL-C, very low-density lipoprotein cholesterol; ox-LDL, oxidized low-density lipoprotein.

Table II. SOD and MDA levels in peripheral blood serum of mice in each group.

Group	n	SOD (U/ml)	MDA (nmol/ml)
Control	6	268.44±4.19	13.86±0.94
Model	6	245.66±7.03[a]	17.18±0.58[a]
Fisetin	6	260.53±6.28[b]	15.01±1.42[b]
Atorvastatin	6	261.49±8.69[b]	14.94±0.79[b]

Data are presented as mean ± SD. [a]P<0.001 vs. control; [b]P<0.01 vs. model. SOD, superoxide dismutase; MDA, malondialdehyde.

Table III. ALT and AST activities in peripheral blood serum of mice in each group.

Group	n	ALT (U/l)	AST (U/l)
Control	6	19.97±2.93	23.85±4.02
Model	6	72.06±5.38[a]	58.42±5.76[a]
Fisetin	6	25.24±5.00[b]	29.09±4.08[b]
Atorvastatin	6	24.02±4.37[b]	25.76±3.43[b]

Data are presented as the mean ± SD. [a]P<0.001 vs. control; [b]P<0.001 vs. model. ALT, alanine aminotransferase; AST, aspartate aminotransferase.

were no significant differences between the fisetin group and the atorvastatin group (P>0.05; Fig. 1A and B).

Detection of aortic sinus lipid accumulation. Compared with the control group, an increased amount of red-stained lipids were indicated in the aortic sinus of the model group (P<0.001; Fig. 2A and B). However, the mice in the fisetin group and atorvastatin group exhibited significantly decreased lipid accumulation compared with the model group (P<0.001; Fig. 2A and B). There were no significant differences in lipid accumulation between the fisetin group and atorvastatin group (P>0.05; Fig. 2A and B).

Detection of aortic sinus collagen content. The atherosclerotic plaques in the model group were observed to exhibit a thinner fibrous cap and decreased collagen fiber components compared with the control group (P<0.001; Fig. 3A and B). Following fisetin and atorvastatin treatment, collagen fiber content in the atherosclerotic plaques of the aortic sinus increased compared with the model group and were distributed evenly (P<0.001; Fig. 3A and B). There were no significant differences between collagen fiber content in the fisetin group and the atorvastatin group (P>0.05; Fig. 3A and B).

Aortic expression of PCSK9, LOX-1, p53, p21 and p16. Compared with the control group, the expressions of PCSK9 (P<0.01; Fig. 4A and F), LOX-1 (P<0.001; Fig. 4B and F), p53 (P<0.05; Fig. 4C and F), p21 (P<0.01; Fig. 4D and F), and p16 (P<0.001; Fig. 4E and F) significantly increased in the model group. Following fisetin and atorvastatin treatment, the expressions of PCSK9 (P<0.001; Fig. 4A and F), LOX-1 (P<0.01, P<0.001; Fig. 4B and F), p53 (P<0.05; Fig. 4C and F), p21 (P<0.001; Fig. 4D and F) and p16 (P<0.001; Fig. 4E and F) significantly decreased compared with the model group. There were no significant differences between PCSK9, LOX-1, p53, p21 and p16 expressions in the fisetin group and the atorvastatin group (P>0.05; Fig. 4A-F).

Discussion

AS is mainly characterized by the accumulation of a large amount of lipids in the arterial wall, and disorders of lipid metabolism are a risk factor for AS (14). PCSK9 is a serine protease, and its functional mutation has been positively correlated with plasma LDL-C concentration in patients with familial hypercholesterolemia (15). A previous report demonstrated that the overexpression of PCSK9 in C57BL/6 mice that were fed a high-fat diet led to the rapid formation of hyperlipidemia and aggravated the pathological changes of AS (16). In contrast, knockout of PCSK9 in $Ldlr^{-/-}$ $Apobec1^{-/-}$ mice has been revealed to increase the levels of serum lipids, including TC, TG and cholesterol ester, free cholesterol and the production and secretion of apoB (17). Administration of a PCSK9 inhibitor (human monoclonal antibody RG7652) has also been indicated to reduce the levels of plasma LDL and VLDL and increase the level of HDL in patients with coronary heart disease (18). LOX-1 is essential for the pathogenesis of AS, including renal dysfunction, endothelial cell apoptosis and senescence, mediated foam cell formation and regulation of collagen accumulation in AS plaques (19). Overexpression of

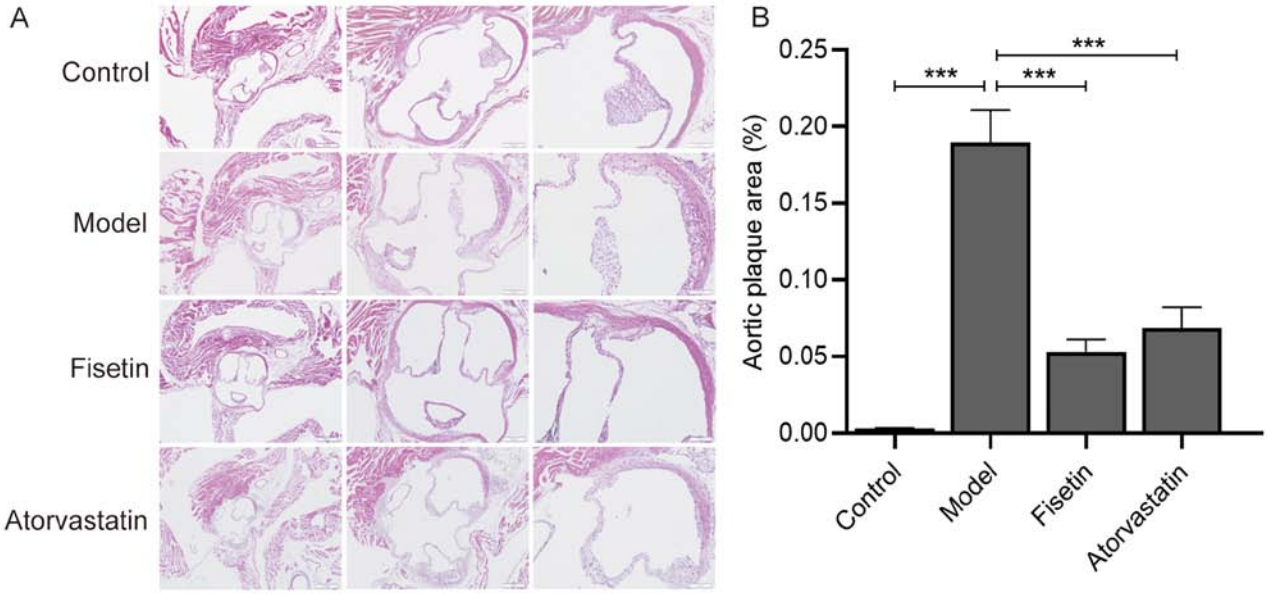

Figure 1. Effect of fisetin on the aortic plaque area in apoE$^{-/-}$ mice. (A) Hematoxylin and Eosin staining. Magnification, x40 (first column), x100 (second column) and x200 (third column). (B) Percentage of aortic plaque area. Data are presented as mean ± SD (n=6). One-way ANOVA of variance tests followed by least significant difference test was performed for comparison of two or more groups. ***P<0.001.

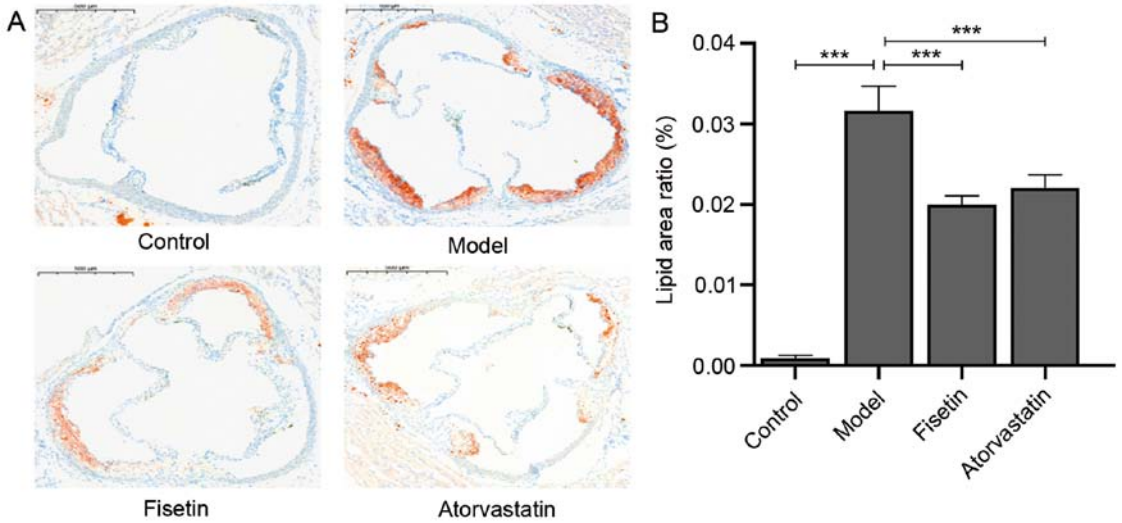

Figure 2. Effect of fisetin on relative area of apoE$^{-/-}$ mice aortic plaque lipid accumulation. (A) Oil red O staining. Magnification, x40. Scale bar, 500 μm. (B) Percentage of red-stained lipid area. Data are presented as mean ± SD (n=6). One-way ANOVA of variance tests followed by least significant difference test was performed for comparison of two or more groups. ***P<0.001.

endothelium-specific LOX-1 in apoE$^{-/-}$ mice has been indicated to increase aortic fat stripe formation and macrophage recruitment as well as accelerate the formation and development of AS plaque (20). After the targeted inhibition of LOX-1 by miRNA-98, the foam and lipid deposition of peritoneal macrophages in apoE$^{-/-}$ mice has been demonstrated to decrease (21). Overexpressed PCSK9 in mouse peritoneal macrophages can promote the expression of LOX-1 and increase the uptake of ox-LDL, thus promoting the progression of AS (22). In human aortic ECs and SMCs exposed to lipopolysaccharide, the expression of LOX-1 has been revealed to decrease in ECs and SMCs with silenced PCSK9 as well as in PCSK9$^{-/-}$ mice (7). In the current study, the AS model induced by high-fat diet in apoE$^{-/-}$ mice was successfully established, which included increased AS plaque and lipid accumulation in the aortic sinus as well as decreased collagen content. Compared with the control group, serum lipid analysis in the peripheral blood of mice revealed that the levels of TC, LDL-C, VLDL-C and ox-LDL increased, whereas the level of HDL-C decreased, and the expressions of PCSK9 and LOX-1 increased in the aorta of mice.

AS is closely associated with aging and often occurs in middle-aged and elderly individuals (23). In the pathological process of AS, peroxides produced by oxidative stress can cause damage to DNA, protein and other cell components, and can lead to vascular endothelial dysfunction (24). SOD and MDA are associated with oxidative damage, which can reflect the severity of cells attacked by free radicals and the

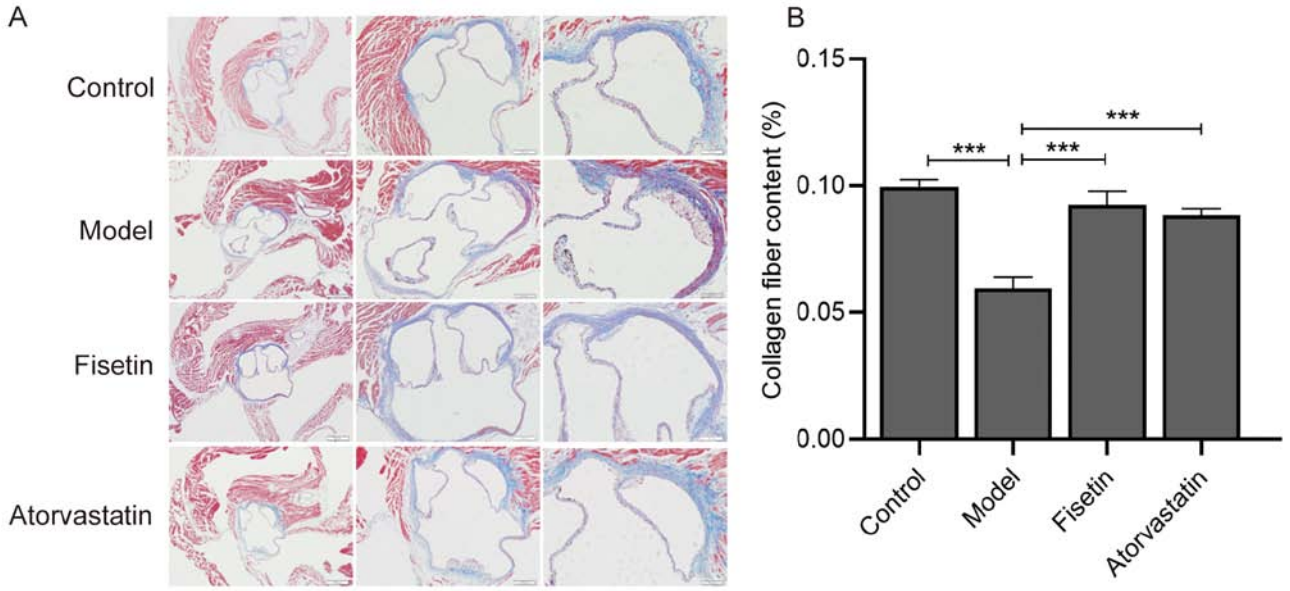

Figure 3. Effect of fisetin on the content of collagen fiber in aortic sinus of apoE$^{-/-}$ mice. (A) Masson staining. Magnification, x40 (first column), x100 (second column) and x200 (third column). (B) Percentage of collagen content. Data are presented as mean ± SD (n=6). One-way ANOVA of variance tests followed by least significant difference test was performed for comparison of two or more groups. ***P<0.001.

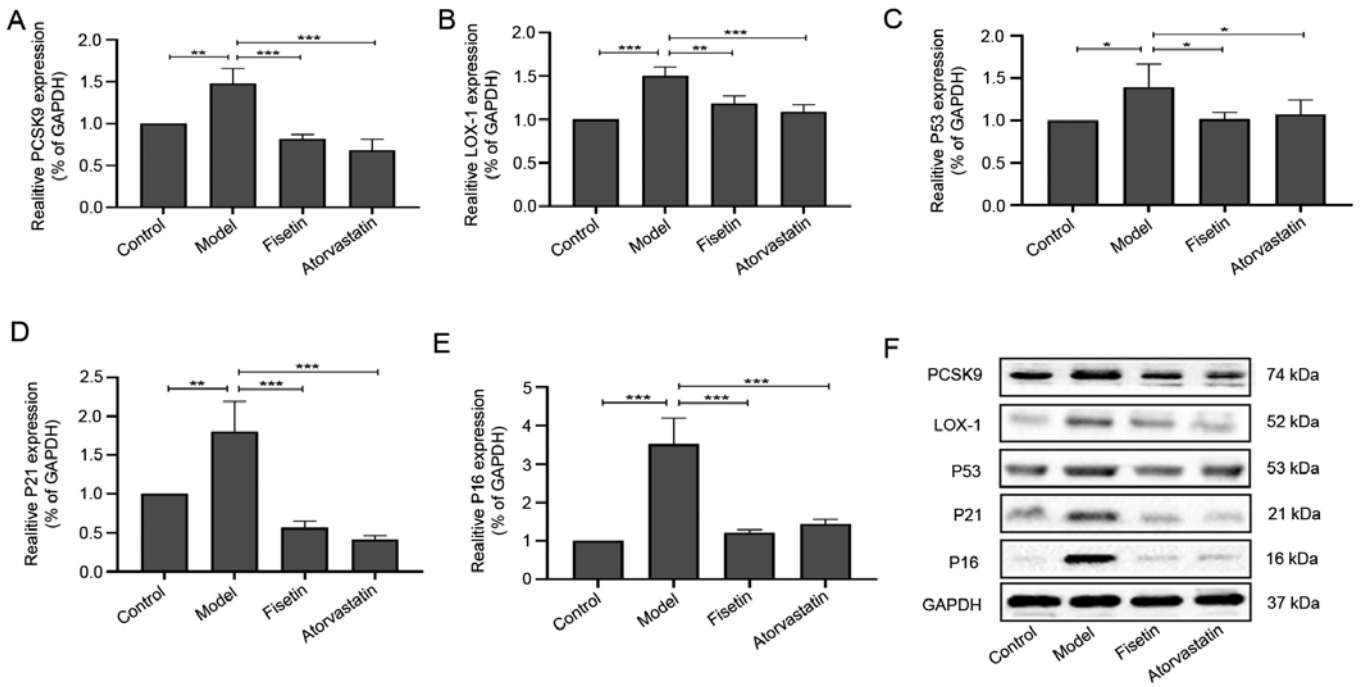

Figure 4. Effect of fisetin on the expression levels of PCSK9, LOX-1, p53, p21 and p16 in apoE$^{-/-}$ mice aorta. Expression levels of (A) PCSK9, (B) LOX-1, (C) p53, (D) p21 and (E) p16. (F) Western blot analysis results for PCSK9, LOX-1, p53, p21 and p16 expressions in the mouse aorta. Data are presented as mean ± SD (n=3). One-way ANOVA of variance tests followed by least significant difference test was performed for comparison of two or more groups, *P<0.05, **P<0.01, ***P<0.001. PCSK9, proprotein convertase subtilisin/kexin type 9; LOX-1, lectin-like oxidized low-density lipoprotein receptor-1; p53, tumor suppressor protein p53; p21, cyclin-dependent kinase inhibitor 1A; p16, multiple tumor suppressor-1.

ability of scavenging oxygen free radicals (25,26). As an antioxidant enzyme for scavenging free radicals in the body, SOD can scavenge free radicals that can destroy the cells of the body (25). MDA is the end product of lipid peroxides, and its accumulation can cause nucleic acid destruction and protein denaturation, thus promoting cell senescence (26). P53, p21 and p16 are aging markers that regulate the cell cycle and apoptosis and participate in the pathway of cell senescence (6). The oxidative stress-mediated p53/p21 signaling pathway can promote the senescence of human aortic ECs and activate p16 transcription, thus aggravating AS lesions (27). In addition to participating in lipid metabolism, PCSK9 serves an important role in the process of vascular aging and is directly associated with the occurrence and

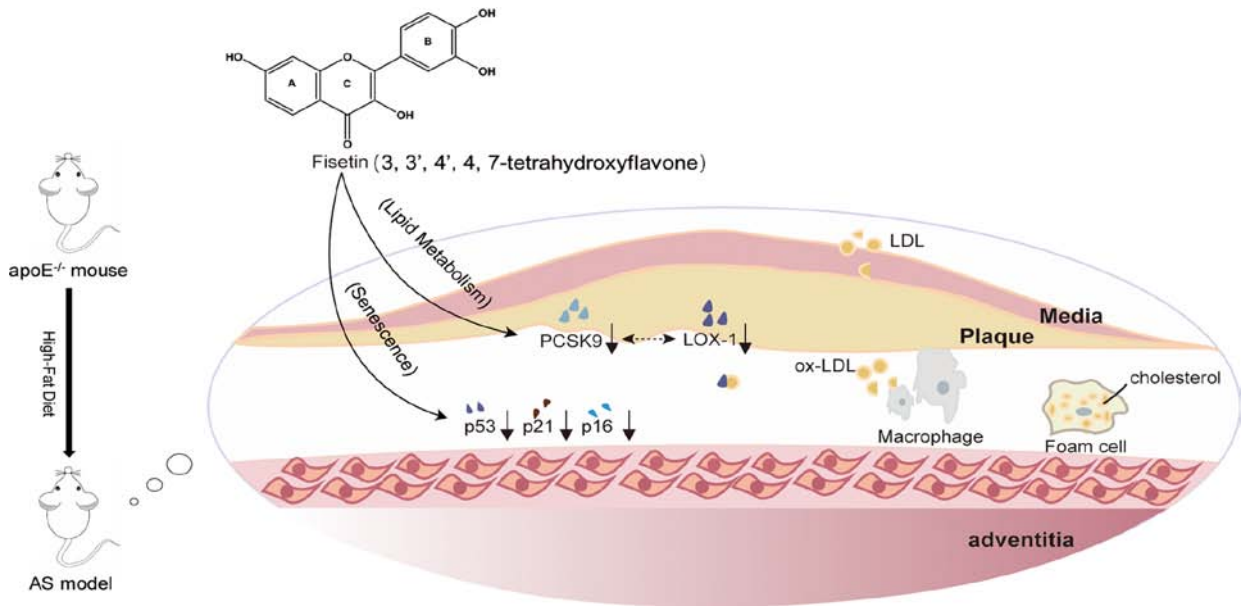

Figure 5. Schematic summary of how fisetin exerts an anti-AS effect in apoE$^{-/-}$ mice fed with a high-fat diet. Fisetin treatment ameliorated lipid accumulation in the atherosclerotic plaque by downregulating PCSK9 and LOX-1, which reduces the uptake of ox-LDL by macrophages, thereby reducing foam cell formation. Fisetin also improves senescence by downregulating the aging-related proteins p53, p21, and p16 in aortic tissue. AS, Atherosclerosis; PCSK9, proprotein convertase subtilisin/kexin type 9; LOX-1, lectin-like oxidized low-density lipoprotein receptor-1; ox-LDL, oxidized low-density lipoprotein; p53, tumor suppressor protein p53; p21, cyclin-dependent kinase inhibitor 1A; p16, multiple tumor suppressor-1.

development of AS (8). It has been reported that PCSK9 is closely associated with brain cholesterol level and nerve cell apoptosis (28). LOX-1 can promote the senescence of mouse cardiac fibroblasts and increase sensitivity to apoptosis (29). Furthermore, overexpression of PCSK9 and LOX-1 in human ECs and SMCs is associated with increased production of mitochondrial ROS (mtROS), whereas knockout of PCSK9 or LOX-1 is associated with a decrease of mtROS (4). In the present study, the model group exhibited a decreased level of serum SOD and an increased level of MDA in the peripheral blood serum of mice. Additionally, the expressions of p53, p21, and p16 were increased in the model group compared with the control group.

As aforementioned, fisetin is a flavonol compound that regulates lipid metabolism disorders, and anti-aging and anti-oxidation activities (30-32). A previous research has demonstrated that fisetin can inhibit the binding of ox-LDL to class B scavenger receptor cluster of differentiation 36 on macrophages and reduce foam cell formation to provide anti-AS effects (33). Fisetin can also inhibit adipose differentiation by reducing mTORC1 activity, thereby reducing adipocyte formation and fat accumulation (34). Moreover, fisetin can reduce the effect of ox-LDL in ECs to improve endothelial dysfunction by downregulating the Erk-5/Mef2c/KLF2 signaling pathway (35). According to a previous report, hypercholesterolemic rats treated with fisetin exhibited significantly decreased plasma TC and LDL-C levels (36). In mice with alcoholic liver injury, fisetin reduced the levels of TG and free fatty acid as well as the number of lipid droplets (37). Fisetin also significantly decreased the plasma levels of TC, TG, LDL-C and VLDL-C, and increased the level of HDL-C in diabetic rats (38). In addition, fisetin serves an anti-aging role by inhibiting the proliferation of senescent cells (39). Fisetin has also been revealed to significantly improve cognitive and motor dysfunction and brain inflammation in SAMP8 aging mice (40), and effectively maintain the redox homeostasis of erythrocytes in aging rats (41). Fisetin can prolong the life span of yeast, nematode, drosophila melanogaster and mice (42). Furthermore, fisetin can be used as a cardioprotective agent; a dose of 10 mg/kg was previously revealed to significantly reduce the cardiotoxicity induced by doxorubicin in rats (43). Fisetin also exhibits protective effects on cerebral nerves, and at doses of 25 and 74 mg/kg, can be rapidly distributed in cerebral vessels and brain parenchyma of mice via intragastric or intraperitoneal injection (44). Fisetin is the main chemical component of Lacqueraceae, and its water extract (200 mg/kg) exhibits no obvious anatomical changes or tissue damage and hepatorenal function insufficiency in BALB/C mice; however, a high concentration may inhibit bone marrow hematopoiesis long-term (45). The current study demonstrated that fisetin could significantly decrease the serum levels of TC, LDL-C, VLDL-C and ox-LDL, and the detection of ALT and AST activities in the peripheral blood serum of mice suggested that the fisetin dosage was within a safe range (Table III).

In summary, the current study concluded that fisetin exerted an anti-AS effect in apoE$^{-/-}$ mice fed with a high-fat diet, which reduced the area of atherosclerotic plaques and lipid accumulation and increased the collagen fiber content in the aortic sinus. In addition, fisetin treatment resulted in decreased levels of TC, LDL-C, VLDL-C, ox-LDL and MDA, and increased the level of SOD compared with the control group. Finally, fisetin treatment resulted in the downregulation of PCSK9, LOX-1, p53, p21 and p16 protein expression in aortic tissue, compared with the model group. Combined with the results of previous *in vitro* experiments, these results suggested that fisetin may serve an atheroprotective role, ameliorating abnormal lipid metabolism by regulating the expression of PCSK9 and LOX-1, and improving senescence by regulating the expressions of p53, p21 and p16 (Fig. 5).

Acknowledgements

Not applicable.

Funding

The current study was supported by the National Natural Science Foundation of China (grant no. 81873348), the National Traditional Chinese Medicine Innovation Talent Training Project [Letter (2019) no. 128], and Shanghai University of Traditional Chinese Medicine graduate 'Innovation Ability Training' special research project (grant no. Y201934).

Availability of data and materials

All data generated or analyzed during this study are included in this published article.

Authors' contributions

DS, LY and QJ conceived the experiments and experimental plan. LY, QJ and HC performed the experiments and collected the data. LY, QJ, HC, SX, YH and CC analyzed the data. LY and QJ wrote the manuscript. DS, HC, CC, SX and YH reviewed the manuscript critically for important intellectual content. All authors read and approved the final manuscript.

Ethics approval and consent to participate

All animal experiments were approved and carried out in strict compliance with the Animal Care and Use Committee of Shanghai Model Organisms Center, Inc. (IACUC no. 2019-0008).

Patient consent for publication

Not applicable.

Competing interests

The authors declare that they have no competing interests.

References

1. Wang H, Fu H, Zhu R, Wu X, Ji X, Li X, Jiang H, Lin Z, Tang X, Sun S, *et al*: BRD4 contributes to LPS-induced macrophage senescence and promotes progression of atherosclerosis-associated lipid uptake. Aging (Albany NY) 12: 9240-9259, 2020.
2. Del Pinto R, Grassi D, Properzi G, Desideri G and Ferri C: Low density lipoprotein (LDL) cholesterol as a causal role for atherosclerotic disease: Potential role of PCSK9 inhibitors. High Blood Press Cardiovasc Prev 26: 199-207, 2019.
3. Tian K, Ogura S, Little, PJ, Xu SW and Sawamura T: Targeting LOX-1 in atherosclerosis and vasculopathy: Current knowledge and future perspectives. Ann N Y Acad Sci 1443: 34-53, 2019.
4. Ding Z, Liu S, Wang X, Deng X, Fan Y, Shahanawaz J, Shmookler Reis RJ, Varughese KI, Sawamura T and Mehta JL: Cross-talk between LOX-1 and PCSK9 in vascular tissues. Cardiovasc Res 107: 556-567, 2015.
5. Kattoor AJ, Pothineni NVK, Palagiri D and Mehta JL: Oxidative stress in atherosclerosis. Curr Atheroscler Rep 19: 42, 2017.
6. Shimizu I and Minamino T: Cellular senescence in cardiac diseases. J Cardiol 74: 313-319, 2019.
7. Ding Z, Liu S, Wang X, Deng X, Fan Y, Sun C, Wang Y and Mehta JL: Hemodynamic shear stress via ROS modulates PCSK9 expression in human vascular endothelial and smooth muscle cells and along the mouse aorta. Antioxid Redox Signal 22: 760-771, 2015.
8. Grobelna MK, Strauss E and Krasiński Z: The role of proprotein convertase subtilisin-kexin type 9 (PCSK9) in the vascular aging process-is there a link? Kardiochir Torakochirurgia Pol 16: 128-132, 2019.
9. Pal HC, Pearlman RL and Afaq F: Fisetin and Its role in chronic diseases. Adv Exp Med Biol 928: 213-244, 2016.
10. Jin T, Kim OY, Shin MJ, Choi EY, Lee SS, Han YS and Chung JH: Fisetin up-regulates the expression of adiponectin in 3T3-L1 adipocytes via the activation of silent mating type information regulation 2 homologue 1 (SIRT1)-deacetylase and peroxisome proliferator-activated receptors (PPARs). J Agric Food Chem 62: 10468-10474, 2014.
11. Shi YS, Li CB, Li XY, Wu J, Li Y, Fu X, Zhang Y and Hu WZ: Fisetin attenuates metabolic dysfunction in mice challenged with a high-fructose diet. J Agric Food Chem 66: 8291-8298, 2018.
12. Yousefzadeh MJ, Zhu Y, McGowan SJ, Angelini L, Fuhrmann-Stroissnigg H, Xu M, Ling YY, Melos KI, Pirtskhalava T, Inman CL, *et al*: Fisetin is a senotherapeutic that extends health and lifespan. EBioMedicine 36: 18-28, 2018.
13. Jia Q, Cao H, Shen D, Yan L, Chen C and Xing S: Fisetin, via CKIP-1/REGγ, limits oxidized LDL-induced lipid accumulation and senescence in RAW264.7 macrophage-derived foam cells. Eur J Pharmacol 865: 172748, 2019.
14. Summerhill VI, Grechko AV, Yet SF, Sobenin IA and Orekhov AN: The atherogenic role of circulating modified lipids in atherosclerosis. Int J Mol Sci 20: 3561, 2019.
15. Wu NQ and Li JJ: PCSK9 gene mutations and low-density lipoprotein cholesterol. Clin Chim Acta 431: 148-153, 2014.
16. Kumar S, Kang DW, Rezvan A and Jo H: Accelerated atherosclerosis development in C57Bl6 mice by overexpressing AAV-mediated PCSK9 and partial carotid ligation. Lab Invest 97: 935-945, 2017.
17. Sun H, Krauss RM, Chang JT and Teng BB: PCSK9 deficiency reduces atherosclerosis, apolipoprotein B secretion, and endothelial dysfunction. J Lipid Res 59: 207-223, 2018.
18. Hilvo M, Simolin H, Metso J, Ruuth M, Öörni K, Jauhiainen M, Laaksonen R and Baruch A: PCSK9 inhibition alters the lipidome of plasma and lipoprotein fractions. Atherosclerosis 269: 159-165, 2018.
19. Xu S, Ogura S, Chen J, Little PJ, Moss J and Liu P: LOX-1 in atherosclerosis: Biological functions and pharmacological modifiers. Cell Mol Life Sci 70: 2859-2872, 2013.
20. Akhmedov A, Rozenberg I, Paneni F, Camici GG, Shi Y, Doerries C, Sledzinska A, Mocharla P, Breitenstein A, Lohmann C, *et al*: Endothelial overexpression of LOX-1 increases plaque formation and promotes atherosclerosis in vivo. Eur Heart J 35: 2839-2848, 2014.
21. Dai Y, Wu X, Dai D, Li J and Mehta JL: MicroRNA-98 regulates foam cell formation and lipid accumulation through repression of LOX-1. Redox Biol 16: 255-262, 2018.
22. Ding Z, Liu S, Wang X, Theus S, Deng X, Fan Y, Zhou S and Mehta JL: PCSK9 regulates expression of scavenger receptors and ox-LDL uptake in macrophages. Cardiovasc Res 114: 1145-1153, 2018.
23. Fajemiroye JO, da Cunha LC, Saavedra-Rodríguez R, Rodrigues KL, Naves LM, Mourão AA, da Silva EF, Williams NEE, Martins JLR, Sousa RB, *et al*: Aging-induced biological changes and cardiovascular diseases. Biomed Res Int 2018: 7156435, 2018.
24. Dzięgielewska-Gęsiak S, Płóciniczak A, Wilemska-Kucharzewska K, Kokot T, Muc-Wierzgoń M and Wysocka E: The relationship between plasma lipids, oxidant-antioxidant status, and glycated proteins in individuals at risk for atherosclerosis. Clin Interv Aging 14: 789-796, 2019.
25. Wang Y, Branicky R, Noë A and Hekimi S: Superoxide dismutases: Dual roles in controlling ROS damage and regulating ROS signaling. J Cell Biol 217: 1915-1928, 2018.
26. Papac-Milicevic N, Busch CJ and Binder CJ: Malondialdehyde epitopes as targets of immunity and the implications for atherosclerosis. Adv Immunol 131: 1-59, 2016.
27. Zhou Z, Yin Y, Chang Q, Sun G and Dai Y: Downregulation of B-myb promotes senescence via the ROS-mediated p53/p21 pathway, in vascular endothelial cells. Cell Prolif 50: e12319, 2017.

28. Adorni MP, Ruscica M, Ferri N, Bernini F and Zimetti F: Proprotein convertase subtilisin/kexin type 9, brain cholesterol homeostasis and potential implication for Alzheimer's disease. Front Aging Neurosci 11: 120, 2019.
29. Wang X, Khaidakov M, Ding Z, Dai Y, Mercanti F and Mehta JL: LOX-1 in the maintenance of cytoskeleton and proliferation in senescent cardiac fibroblasts. J Mol Cell Cardiol 60: 184-190, 2013.
30. Gaballah HH, El-Horany HE and Helal DS: Mitigative effects of the bioactive flavonol fisetin on high-fat/high-sucrose induced nonalcoholic fatty liver disease in rats. J Cell Biochem 120: 12762-12774, 2019.
31. Singh S, Singh AK, Garg G and Rizvi SI: Fisetin as a caloric restriction mimetic protects rat brain against aging induced oxidative stress, apoptosis and neurodegeneration. Life Sci 193: 171-179, 2018.
32. Zhang L, Wang H, Zhou Y, Zhu Y and Fei M: Fisetin alleviates oxidative stress after traumatic brain injury via the Nrf2-ARE pathway. Neurochem Int 118: 304-313, 2018.
33. Lian TW, Wang L, Lo YH, Huang IJ and Wu MJ: Fisetin, morin and myricetin attenuate CD36 expression and oxLDL uptake in U937-derived macrophages. Biochim Biophys Acta 1781: 601-609, 2008.
34. Jung CH, Kim H, Ahn J, Jeon TI, Lee DH and Ha TY: Fisetin regulates obesity by targeting mTORC1 signaling. J Nutr Biochem 24: 1547-1554, 2013.
35. Patel R, Varghese JF, Singh RP and Yadav UCS: Induction of endothelial dysfunction by oxidized low-density lipoproteins via downregulation of Erk-5/Mef2c/KLF2 signaling: Amelioration by fisetin. Biochimie 163: 152-162, 2019.
36. Shin MJ, Cho Y, Moon J, Jeon HJ, Lee SM and Chung JH: Hypocholesterolemic effect of daily fisetin supplementation in high fat fed sprague-dawley rats. Food Chem Toxicol 57: 84-90, 2013.
37. Sun Q, Zhang W, Zhong W, Sun X and Zhou Z: Dietary fisetin supplementation protects against alcohol-induced liver injury in mice. Alcohol Clin Exp Res 40: 2076-2084, 2016.
38. Prasath GS and Subramanian SP: Antihyperlipidemic effect of fisetin, a bioflavonoid of strawberries, studied in streptozotocin-induced diabetic rats. J Biochem Mol Toxicol 28: 442-449, 2014.
39. Zhu Y, Doornebal EJ, Pirtskhalava T, Giorgadze N, Wentworth M, Fuhrmann-Stroissnigg H, Niedernhofer LJ, Robbins PD, Tchkonia T and Kirkland JL: New agents that target senescent cells: The flavone, fisetin, and the BCL-XL inhibitors, A1331852 and A1155463. Aging (Albany NY) 9: 955-963, 2017.
40. Currais A, Farrokhi C, Dargusch R, Armando A, Quehenberger O, Schubert D and Maher P: Fisetin reduces the impact of aging on behavior and physiology in the rapidly aging SAMP8 mouse. J Gerontol A Biol Sci Med Sci 73: 299-307, 2018.
41. Singh S, Garg G, Singh AK, Bissoyi A and Rizvi SI: Fisetin, a potential caloric restriction mimetic, attenuates senescence biomarkers in rat erythrocytes. Biochem Cell Biol 97: 480-487, 2019.
42. Wood JG, Rogina B, Lavu S, Howitz K, Helfand SL, Tatar M and Sinclair D: Sirtuin activators mimic caloric restriction and delay ageing in metazoans. Nature 430: 686-689, 2004.
43. Ma T, Kandhare AD, Mukherjee-Kandhare AA and Bodhankar SL: Fisetin, a plant flavonoid ameliorates doxorubicin-induced cardiotoxicity in experimental rats: The decisive role of caspase-3, COX-II, cTn-I, iNOs and TNF-α. Mol Biol Rep 46: 105-118, 2019.
44. Krasieva TB, Ehren J, O'Sullivan T, Tromberg BJ and Maher P: Cell and brain tissue imaging of the flavonoid fisetin using label-free two-photon microscopy. Neurochem Int 89: 243-248, 2015.
45. Varela-Rodríguez L, Sánchez-Ramírez B, Rodríguez-Reyna IS, Ordaz-Ortiz JJ, Chávez-Flores D, Salas-Muñoz E, Osorio-Trujillo JC, Ramos-Martínez E and Talamás-Rohana P: Biological and toxicological evaluation of Rhus trilobata Nutt. (Anacardiaceae) used traditionally in Mexico against cancer. BMC Complement Altern Med 19: 153, 2019.